

Polyp Shape Recovery using Vascular Border from Single Colonoscopy Image

Hiroyasu Usami¹, Yuji Iwahori¹, M. K. Bhuyan², Aili Wang³, Naotaka Ogasawara⁴
and Kunio Kasugai⁴

¹*Department of Computer Science, Chubu University, Kasugai, Japan*

²*Department of Electronics and Electrical Engineering, Indian Institute of Technology Guwahati, Guwahati, India*

³*Higher Education Key Lab., Harbin University of Science and Technology, Harbin, China*

⁴*Department of Gastroenterology, Aichi Medical University, Nagakute, Japan*

Keywords: Shape from Shading, Lambertian Surface, Specular Removal, U-net, RANSAC, Colonoscopy.

Abstract: The shape and size of a colonic polyp is a biomarker that correlates with its risk of malignancy and guides its clinical management. It is the most accurate method for detecting polyps of all sizes, and it allows biopsy of lesions and resection of most polyps, and it is considered nowadays as the gold standard for colon screening. However, there are still open challenges to overcome, such as the reduction of the missing rate. Colonoscopy images usually consist of nonrigid objects such as a polyp, and no approaches have been proposed to recovery shape and absolute size from a single image. Hence, it is a challenging topic to reconstruct polyp shape using computer vision technique. This paper proposes a polyp shape retrieval method based on Shape from Shading (SFS), and this research contributes to mitigating constraint for applying SFS to the single colonoscopy image using vascular border information. Experiments confirmed that the proposed method recovered approximate polyp shapes.

1 INTRODUCTION

A polyp guideline for the diagnosis, treatment, and surveillance for patients with colorectal polyps published originally in 1993(Bond, 1993), and it has been developing following evidence-based(Force, 1989)(Winawer et al., 1997)(Byers et al., 1997). The guideline indicates that the shape and size of a colonic polyp is a biomarker that correlates with its risk of malignancy and guides its clinical management.

Endoscopy images usually consist of nonrigid objects such as a polyp so that applying photoclinometry based recovery approach is reasonable for the issue mentioned earlier. Shape from Shading (SFS)(Horn, 1989) is as one valuable approach based on photoclinometry. SFS uses the intensity of images directly to reconstruct the target object surface orientation from a single image. Some approaches (Iwahori et al., 2015)(Wu et al., 2010) reconstructed 3D shape from colonoscopy image based on SFS. The paper(Iwahori et al., 2015) proposed a polyp recovery approach using both photometric and geometric constraints assuming one light source colonoscopy. Another ap-

proach(Usami et al., 2016) reconstructed polyp shape considering more actual colonoscopy, which has two light sources, and it used a neural network to modify the obtained surface gradients. In case of besides targeting polyp, the paper (Wu et al., 2010) proposed a 3D shape recovery method for an artificial spine.

SFS and colonoscopy image are compatible on the first sight, but there are constraints for applying SFS to colonoscopy image. Those approaches need some parameters like a depth Z from colonoscopy lens to the surface, and surface reflectance coefficient C . Furthermore, those approaches assume the whole surface which has same the C and the Lambertian surface. This research contributes mitigating constraint for applying SFS to the colonoscopy regardless of generating Lambertian image processing based on vasculature structure and its border. The outline of this paper is as follows. Firstly, an assumed observation system and photometric constraints are introduced. In the next, preprocessing and approaches which obtaining parameters using vascular are described for polyp shape retrieval. In the experiment, evaluation is conducted using actual colonoscopy images. Finally,

conclude the proposed approach and discuss future works in conclusion.

2 ALGORITHM

The proposed approach assumes an observation system of two light source colonoscopy for polyp shape recovery, and consists of following steps.

- Step0. Assume an observation system of two light source colonoscopy.
- Step1. Estimate the camera parameters by conducting camera calibration.
- Step2. Conduct specular highlight removal.
- Step3. Conduct blood vessel extraction using U-net.
- Step4. Obtain depth Z and reflectance coefficient C of blood vessels by estimating its horizontal plane, and using its geometric structure.
- Step5. Obtain depth Z and reflectance coefficient C of intestinal-inner-walls using borders between blood vessels and optimization.

2.1 Observation System of Two Light Source Colonoscopy

The observation system of the colonoscopy is assumed to be a point light source and perspective projection. According to the actual environment of the colonoscopy, two light point sources are assumed as shown in Fig.1.

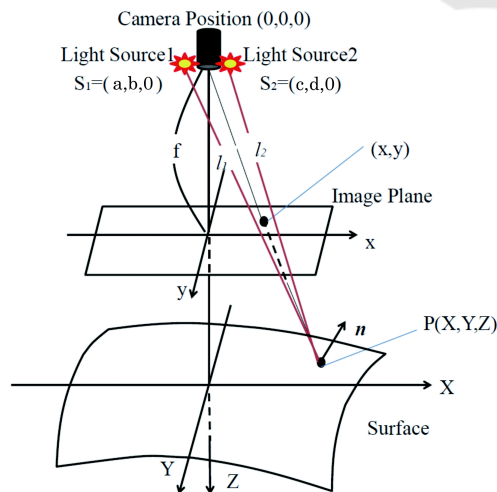


Figure 1: Observation System of Two Light Sources Endoscope.

Here, let the coordinate of the center of the lens be $(0,0,0)$, let both light source coordinate be $\mathbf{s}_1 =$

$(a,b,0)$ and $\mathbf{s}_2 = (c,d,0)$, let f be focal length, let each distance from light source to surface be l_1 and l_2 . Let \mathbf{n} be the normal surface vector. Image intensity E and reflectance coefficient C can be denoted Eq.(1) following illuminance inverse square law.

$$E = C \left(\frac{\mathbf{n} \cdot \mathbf{s}_1}{l_1^2} + \frac{\mathbf{n} \cdot \mathbf{s}_2}{l_2^2} \right) \quad (1)$$

Eq.(1) can be denoted using depth Z from the lens to the surface as following equations. Normal vector \mathbf{n} on arbitrary point of diffuse reflectance surface can be represented Eq.(2).

$$\mathbf{n} = \frac{(p, q, -1)}{\sqrt{p^2 + q^2 + 1}} \quad (2)$$

Here, let each p, q be surface gradient.

$$(p, q) = \left(\frac{\partial Z}{\partial X}, \frac{\partial Z}{\partial Y} \right) \quad (3)$$

Let arbitrary surface point be X, Y, Z , l_1 and l_2 can be represented

$$l_1 = \sqrt{(a-X)^2 + (b-Y)^2 + Z^2} \quad (4)$$

$$l_2 = \sqrt{(c-X)^2 + (d-Y)^2 + Z^2} \quad (5)$$

Both light source vector \mathbf{s}_1 and \mathbf{s}_2 on arbitrary point of diffuse reflectance surface can be denoted as follows.

$$\mathbf{s}_1 = \frac{(a-X, b-Y, -Z)}{\sqrt{(a-X)^2 + (b-Y)^2 + Z^2}} \quad (6)$$

$$\mathbf{s}_2 = \frac{(c-X, d-Y, -Z)}{\sqrt{(c-X)^2 + (d-Y)^2 + Z^2}} \quad (7)$$

World coordinate X, Y are represented by Eq.(8)

$$X = \frac{x}{f}Z, \quad Y = \frac{y}{f}Z \quad (8)$$

Substituting Eq.(2)-Eq.(8) into Eq.(1), E and C can be denoted using Z as Eq.(9).

$$E = \frac{C}{\sqrt{p^2 + q^2 + 1}} \left(\frac{-p(a - \frac{x}{f}Z) - q(b - \frac{y}{f}Z) + Z}{\left((a - \frac{x}{f}Z)^2 + (b - \frac{y}{f}Z)^2 + Z^2 \right)^{\frac{3}{2}}} + \frac{-p(c - \frac{x}{f}Z) - q(d - \frac{y}{f}Z) + Z}{\left((c - \frac{x}{f}Z)^2 + (d - \frac{y}{f}Z)^2 + Z^2 \right)^{\frac{3}{2}}} \right) \quad (9)$$

The proposed method reconstructs the 3D shape from colonoscopy images postulated in the observation model. This Eq.(9) is used to solve each C of the blood vessel and the intestinal-inner-wall (Based on Eq.(16) and Eq.(26)).

2.2 Camera Calibration

Camera parameters of the colonoscopy are estimated. Estimating camera parameters of the colonoscopy is performed using multiple images of checkerboard taken by colonoscopy following existing camera calibration techniques (Zhang, 2000) (Heikkila and Silvén, 1997). Fig.(2) shows examples of checker board image which taken by an colonoscopy is as shown in Fig.(2).

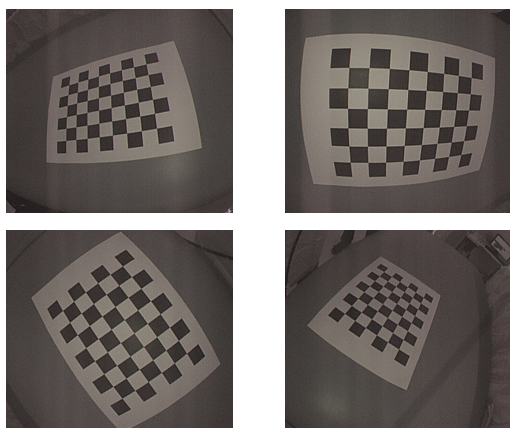


Figure 2: Examples of Checker Board.

Furthermore, positions of two light source on colonoscopy $S_1 = (a, b, 0)$ and $S_2 = (c, d, 0)$ are estimated by conducting optimization for a know sphere object image taken by the colonoscopy.

2.3 Specular Highlight Removal

The spectral energy distribution of the light reflected from the surface can be denoted as the product of the spectral energy distribution of the illumination and the surface reflectance. Following the dichromatic reflection model (Shafer, 1985), the reflected light can be separated into two components specular and diffuse reflection. Specular components affect the result of shape recovery under SFS approach and, frequently arise on the colonoscopy image. The paper (Tchoulack et al., 2008) proposed the specular components removal method on colonoscopy image by conducting the in-painting process to specular components. Modified region by in-painting process lacks the surface information.

The diffuse color component has a characteristic that the maximum fraction of the diffuse color component in diffuse local patches in color images changes smoothly. Hence specular components can be removed by following this characteristic. Furthermore, the proposed approach obtains depth Z and reflectance coefficient C based using the border bet-

ween blood vessels and intestinal-inner-walls. Specular components removal process should be done without removing the border between blood vessel and intestinal-inner-walls since the border information is used when reflectance coefficient C is estimated separately at each region around the border. The proposed approach removes specular components introducing bilateral filter based on the method (Yang et al., 2010) (Yang et al., 2015).

2.4 Blood Vessel Segmentation

The proposed approach obtains depth Z and reflectance coefficient C using blood vessel information. As segmentation methods, some methods were proposed (Carreira and Sminchisescu, 2011) (Uijlings et al., 2013) (Ronneberger et al., 2015). In this case, the desired output should include localization, i.e., a class label is supposed to be assigned to each pixel, and segmentation method should be applicable to vasculature structure. This paper proposes a method based on the U-net architecture (Ronneberger et al., 2015).

The network architecture of the proposed method is shown in Fig.3. The network architecture was constructed with less down sampling layers because the resolution of the targeted colonoscopy images is not high.

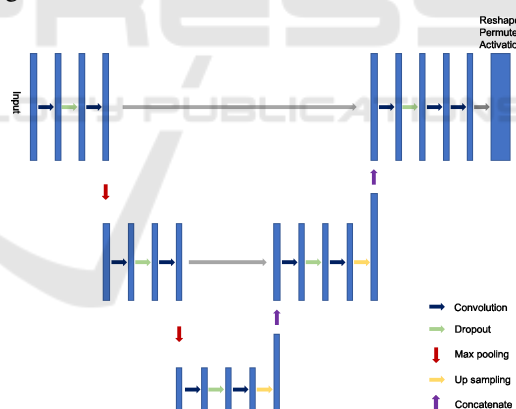


Figure 3: Network Architecture.

The loss function is the cross-entropy and the neural network employs the stochastic gradient descent for optimization. The activation function after each convolutional layer is the Rectifier Linear Unit (ReLU) and dropout of 0.2 are used between two consecutive convolutional layers.

2.5 Obtaining Depth Z and Reflectance Coefficient C

The parameters Z and C for shape recovery under SFS approach are obtained by estimating blood vessel ho-

horizontal plane locally with considering a horizontal plane in the observation system.

2.5.1 Estimation of the Horizontal Plane

The horizontal planes of columnar forms against lens can be obtained by considering the continuity of width from columnar centerline to both end of edge. The columnar width cropped by the horizontal plane against lens as shown in Fig.4 continues while the cropped region are horizon against lens. The horizontal planes of blood vessel can be obtained locally based on this property. The procedure of obtaining the horizontal plane is as follows.

Here, for the explicit description of the algorithm, Fig6 to Fig.9 show the procedure using an example of colonoscopy image with partial blood vessel.

Step1 Extract a blood vessel region in Fig.6 from the original image in Fig.5.

Step2 Extract centerline of the blood vessel by performing line thinning processing as shown in Fig.7.

Step3 Extract edge of blood vessel using morphology operation as shown in Fig.8.

Step4 Draw a line orthogonal to the centerline and crop the line by both end of edge. Finally, extract continuous regions where the cropped line has the same width as shown in Fig.9.

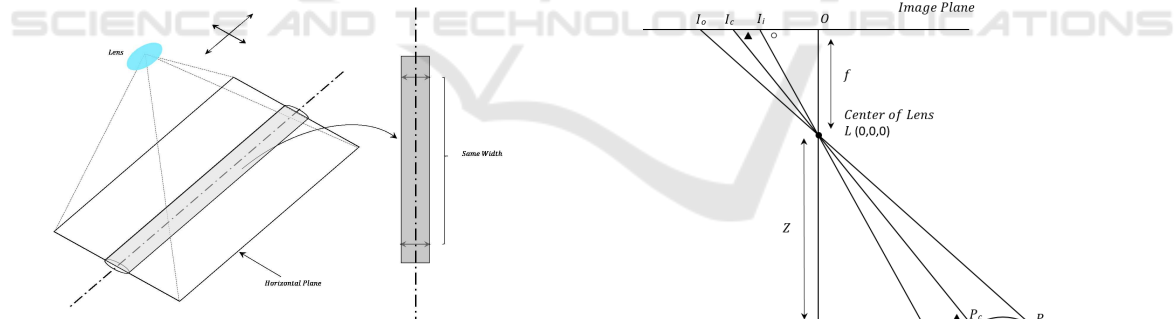


Figure 4: Horizontal Plane of Columnar against lens.

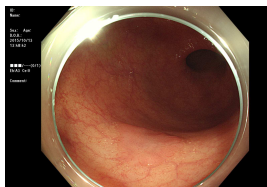


Figure 5: Original Image.



Figure 6: Example of Extracted Blood Vessel Region.



Figure 7: Example of Line Thinning Processing.

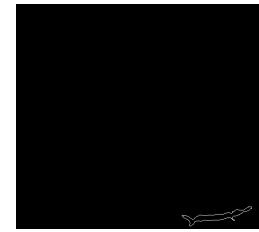


Figure 8: Example of Edge Extraction.

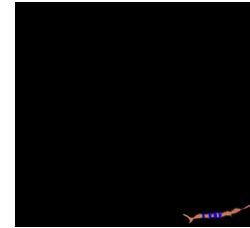


Figure 9: Example of Estimation of Horizontal Plane.

2.5.2 Estimation of Blood Vessel Z and C

Fig.10 shows an observation model for obtaining depth parameter Z of the blood vessel using its horizontal plane.

The depth Z from the colonoscopy lens can be calculated using the model with respect to the estimated horizontal plane of the blood vessel. The procedure for calculating parameter Z is described below.

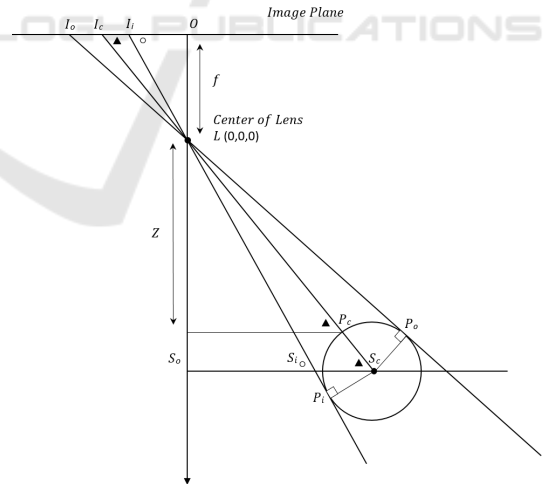


Figure 10: Observation System of Horizontal Plane.

From $\triangle LOI_i \sim \triangle LS_oS_i$ and $\angle LS_iS_o$ is an external angle of $\triangle LS_oS_i$, $\angle LS_iS_c$ can be obtained by Eq.(10).

$$\angle LS_iS_c = \pi - \angle LI_iO \quad (10)$$

From $\triangle LOI_c \sim \triangle LS_oS_c$, $\angle LS_cS_o$ can be expressed from Eq.(11) and Eq.(12).

$$\angle LS_cS_i = \angle LI_cO \quad (11)$$

$$\angle S_i L S_c = \pi - \angle L S_i S_c - \angle L S_c S_i \quad (12)$$

Similarly, $\angle L S_c P_i$ can be obtained from Eq.(13).

$$\angle L S_c P_i = \pi - \frac{\pi}{2} - \angle S_i L S_c \quad (13)$$

The hypotenuse from the lens L to the center of the suture center S_i in $\triangle L S_c S_i$, the distance $L S_c$ can be obtained from Eq.(14). Here, the distance $P_c S_c$ is the same as the radius of blood vessel.

$$L S_c = \frac{P_i S_c}{\cos \angle L S_c P_i} \quad (14)$$

The distance from the lens L to the surface of the blood vessel P_c can be obtained from Eq.(15). Here, $P_c S_c$ is the same as the radius of blood vessel.

$$L P_c = L S_c - P_c S_c \quad (15)$$

From $\triangle L Z P_c \sim \triangle L O I_c$, the depth Z can be obtained from Eq.(16).

$$Z = L P_c \sin \angle L I_c O \quad (16)$$

Here, each surface gradient parameter p , q is obtained stand for the xz plane and the yz plane respectively. The gradient surface parameter p is obtained from a gradient of orthogonal line to the line passing $L = (0, 0)$ and $P_c = (\frac{x_{I_c}}{f} Z, Z)$ on the xz plane. The gradient of the line passing L and P_c is obtained from Eq.(17)

$$\frac{Z}{\frac{x_{I_c}}{f} Z} = \frac{f}{x_{I_c}} \quad (17)$$

The surface gradient p can be obtained from the orthogonal line to the obtained gradient from Eq.(17) as shown in Eq.(18)

$$p = -\frac{x_{I_c}}{f} \quad (18)$$

The gradient surface parameter q is obtained from a gradient of orthogonal line to the line passing $L = (0, 0)$ and $P_c = (\frac{y_{I_c}}{f} Z, Z)$ on the yz plane. The gradient of the line passing L and P_c is obtained from Eq.(19)

$$\frac{Z}{\frac{y_{I_c}}{f} Z} = \frac{f}{y_{I_c}} \quad (19)$$

The surface gradient q can be obtained from the orthogonal line to the obtained gradient from Eq.(19) as shown in Eq.(20)

$$q = -\frac{y_{I_c}}{f} \quad (20)$$

Finally, substituting obtained Z , p , q and image intensity E to Eq.(9), C of the blood vessel is obtained. Here, horizontal plane sections where the same width continues more than 6 tracing the center line of

medical suture were adapted as horizontal plane sections, and calculate MEAN and STD of both Z and C for each section, then, C is selected by the following process. C is confirmed in order from the section where the continuous section of the same width region is long and Z with less STD is obtained, and MEDIAN of C , where the outlier value is not obtained and with the low value of STD, is selected, and Smirnov-Grubbs test(Grubbs et al., 1950) was used for outliers.

2.5.3 Estimation of Intestinal-inner-wall Z and C

Assuming the blood vessel and the intestinal-inner-wall have continuous surface, intestinal-inner-wall parameters Z and C are derived by using the boundary surface as shown in Fig.11.

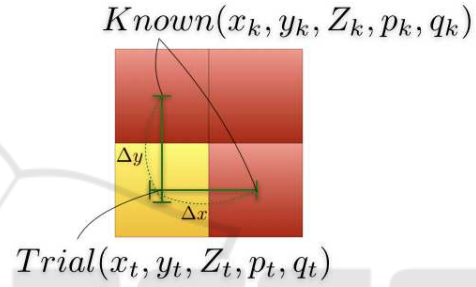


Figure 11: Boundary Surfaces between Blood Vessel and Intestinal-Inner-Wall.

Here, the red color in the figure is defined as a blood vessel region and *Known* point. Let an intestinal-inner-wall neighboring the blood vessel be a *Trial* point. Let a blood vessel point located x axis be a *Known* point K_{BLp} . Let a blood vessel point located y axis be a *Known* point K_{BLq} .

A depth Z of a *Trial* point Z_t and a Z of *Known* point as shown in Eq.(21). Here, $\Delta X = X_t - X_k$, $\Delta Y = Y_t - Y_k$.

$$Z_t = Z_k + p\Delta X + q\Delta Y \quad (21)$$

Each $\Delta X, \Delta Y$ denotes a distance of x axis and y axis respectively on the world coordinate system perspective projection as shown in Eq.(22).

$$Z_t = Z_k + p \left(x_t \frac{Z_t}{f} - x_k \frac{Z_k}{f} \right) + q \left(y_t \frac{Z_t}{f} - y_k \frac{Z_k}{f} \right) \quad (22)$$

Solving Eq.(22) for Z , Eq.(23) can be obtained.

$$Z_t \left(1 - p x_t \frac{1}{f} - q y_t \frac{1}{f} \right) = Z_k \left(1 - p x_k \frac{1}{f} - q y_k \frac{1}{f} \right) \quad (23)$$

Let Z_t be Z_{expect} , the Z_{expect} can be denoted as shown in Eq.(24)

$$Z_{expect} = \frac{Z_k(f - p x_k - q y_k)}{f - p x_t - q y_t} \quad (24)$$

Finally, define $f(p, q, a, b, c, d, f, Z)$ as Eq.(25) using Eq.(9), the surface reflectance coefficient C of intestinal-inner-wall is estimated by optimization using RANSAC (Fischler and Bolles, 1981) and Eq.(26). Here, let p and q be surface gradient, let each light source coordinate be a, b, c, d , let f be focal length, let Z be the calculated depth and let E_i be each real intensity E .

$$f(p, q, a, b, c, d, f, Z) = \frac{1}{\sqrt{p^2 + q^2 + 1}} \left(\frac{-p(a - \frac{x}{f}Z) - q(b - \frac{y}{f}Z) + Z}{((a - \frac{x}{f}Z)^2 + (b - \frac{y}{f}Z)^2 + Z^2)^{\frac{3}{2}}} + \frac{-p(c - \frac{x}{f}Z) - q(d - \frac{y}{f}Z) + Z}{((c - \frac{x}{f}Z)^2 + (d - \frac{y}{f}Z)^2 + Z^2)^{\frac{3}{2}}} \right) \quad (25)$$

$$C^{opt} = \arg \min_C \sum_{i=1}^n ||E_i - Cf(p, q, a, b, c, d, f, Z)|| \quad (26)$$

3 EXPERIMENT

3.1 Camera Calibration

The result of camera calibration is shown in Table.1. The colonoscopy inner parameters as focal length, principal point and radial distortion were obtained by performing camera calibration.

Here, two parameters were obtained respectively because of aspect ratio.

Table 1: Result of Estimation.

Parameter	Result of Calibration
Focal length (pixels)	[718.7447 + / - 0.8387, 718.3827 + / - 0.8654]
Principal point (pixels)	[879.0439 + / - 0.4669, 533.5813 + / - 0.4240]
Radial distortion	[- 0.3913 + / - 0.0010, 0.1178 + / - 0.0008]

Positions of two light source on colonoscopy were estimated using sphere object image taken by the colonoscopy. Positions of two light source estimated are $S_1 = (a : -5.001, b : 1.996, 0)$ and $S_2 = (c : 5.001, d : 1.996, 0)$.

3.2 Blood Vessel Extraction

The vessel probability of each pixel was obtained by averaging multiple predictions to improve the performance. With a stride of 5 pixels in both height and

width, multiple consecutive overlapping patches were extracted in each test image. Then, the vessel probability was obtained for each pixel by averaging probabilities over all the predicted patches covering the pixel.

Evaluation was done using masked images created by manual drawing as ground truth. Fig.12 shows the results of colon blood vessel detection and overall accuracy of the prediction was 0.8432.

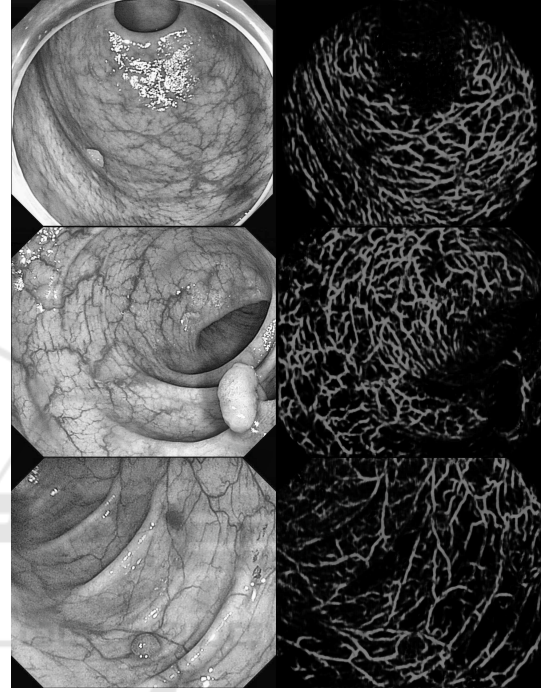


Figure 12: Example of Prediction Results.

Fig.13 shows the Area Under the ROC curve (AUC ROC) of the evaluation, and AUC was 0.9030.

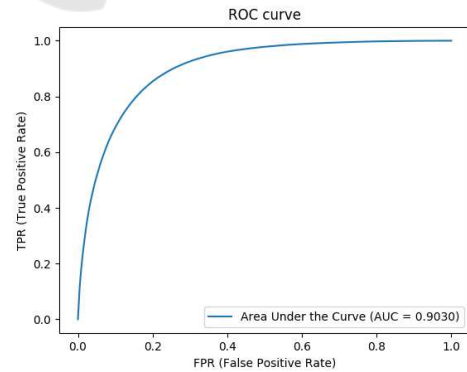


Figure 13: AUC ROC.

From the result of blood vessel extraction, the proposed method extracted blood vessel region accurately.

3.3 Polyp Shape Reconstruction

Using blood vessel information and obtained parameters, polyp shape recovery was performed. There are some obstacles like as body part of the colonoscopy for shape recovery depend on the scene, so that colonoscopy images were cropped for applying the proposed method. Each original colonoscopy image are shown in Fig.14,18,22, selected regions of blood vessel horizontal plane are shown in Fig.15,19,23, shape recovery images are shown in Fig.16,20,24 and size measurement result image are shown in Fig.17,21,25.

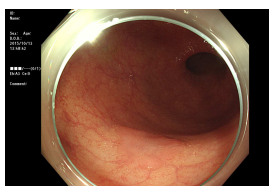


Figure 14: Original Image 1.

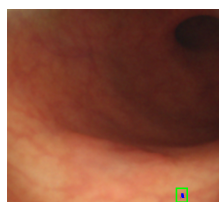


Figure 15: Selected horizontal region for Image 1.

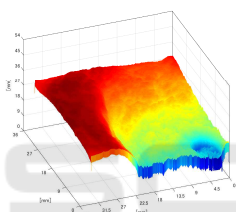


Figure 16: Recovered Shape for Image 1.

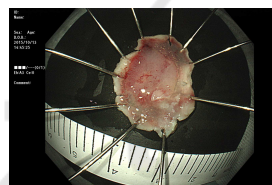


Figure 17: Size Measurement Result in Image 1 after Extraction.

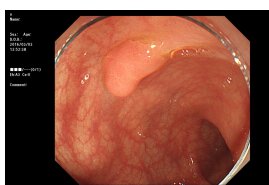


Figure 18: Original Image 2.

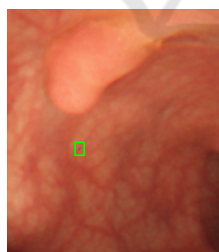


Figure 19: Selected horizontal region for Image 2.

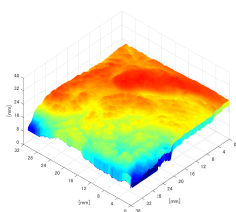


Figure 20: Recovered Shape for Image 2.

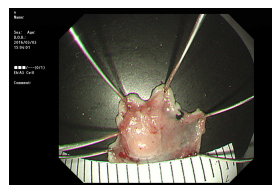


Figure 21: Size Measurement Result for Image 2 after Extraction.

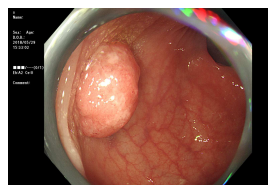


Figure 22: Original Image 3.

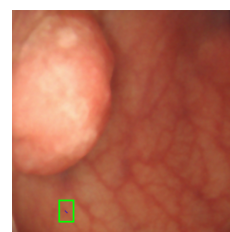


Figure 23: Selected horizontal region for Image 3.

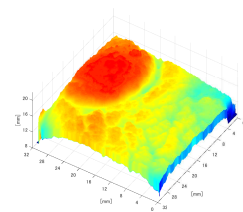


Figure 24: Recovered Shape for Image 3.

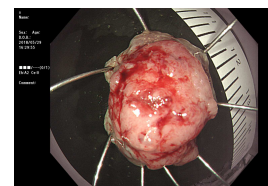


Figure 25: Size Measurement Result for Image 3 after Extraction.

Each C has obtained as 89217, 118153, 23074, respectively. Compared with measured images after extraction and shape recovery result, approximate polyp shape was reconstructed using blood vessel information and obtained parameters.

4 CONCLUSION

This paper proposed a polyp shape recovery method which mitigated the constraint for applying SFS to the colonoscopy image based on the vasculature structure. The proposed approach assumed two light source endoscope according to the actual environment for polyp shape retrieval. Parameters for applying SFS, the camera inner parameters were obtained by conducted camera calibration, depth Z and reflectance coefficient C were obtained by estimating vascular horizontal plane and using its border of neighboring intestinal-inner-walls. From experiments, it is confirmed that the proposed method recovered approximate absolute polyp shape using vascular information and obtained parameters from a single endoscope image. Especially, regardless of generating Lambertian image processing, the proposed method realized polyp shape recovery from a single endoscope image.

ACKNOWLEDGEMENTS

This research is supported by JSPS Grant-in-Aid for Scientific Research (C) (17K00252) and Chubu University Grant.

REFERENCES

- Bond, J. H. (1993). Polyp guideline: diagnosis, treatment, and surveillance for patients with nonfamilial colorectal polyps. *Annals of internal medicine*, 119(8):836–843.
- Byers, T., Levin, B., Rothenberger, D., Dodd, G. D., Smith, R. A., Detection, A. C. S., and on Colorectal Cancer), T. A. G. (1997). American cancer society guidelines for screening and surveillance for early detection of colorectal polyps and cancer: update 1997. *CA: a cancer journal for clinicians*, 47(3):154–160.
- Carreira, J. and Sminchisescu, C. (2011). Cpmc: Automatic object segmentation using constrained parametric min-cuts. *IEEE Transactions on Pattern Analysis & Machine Intelligence*, (7):1312–1328.
- Fischler, M. A. and Bolles, R. C. (1981). A paradigm for model fitting with applications to image analysis and automated cartography (reprinted in readings in computer vision, ed. ma fischler,”. *Comm. ACM*, 24(6):381–395.
- Force, U. P. S. T. (1989). *Guide to clinical preventive services: report of the US Preventive Services Task Force*. DIANE publishing.
- Grubbs, F. E. et al. (1950). Sample criteria for testing outlying observations. *The Annals of Mathematical Statistics*, 21(1):27–58.
- Heikkila, J. and Silvén, O. (1997). A four-step camera calibration procedure with implicit image correction. In *Computer Vision and Pattern Recognition, 1997. Proceedings., 1997 IEEE Computer Society Conference on*, pages 1106–1112. IEEE.
- Horn, B. K. (1989). Obtaining shape from shading information. In *Shape from shading*, pages 123–171. MIT press.
- Iwahori, Y., Tatematsu, K., Nakamura, T., Fukui, S., Woodham, R. J., and Kasugai, K. (2015). 3d shape recovery from endoscope image based on both photometric and geometric constraints. In *Knowledge-Based Information Systems in Practice*, pages 65–80. Springer.
- Ronneberger, O., Fischer, P., and Brox, T. (2015). U-net: Convolutional networks for biomedical image segmentation. In *International Conference on Medical image computing and computer-assisted intervention*, pages 234–241. Springer.
- Shafer, S. A. (1985). Using color to separate reflection components. *Color Research & Application*, 10(4):210–218.
- Tchoulack, S., Langlois, J. P., and Cheriet, F. (2008). A video stream processor for real-time detection and correction of specular reflections in endoscopic images. In *Circuits and Systems and TAISA Conference, 2008. NEWCAS-TAISA 2008. 2008 Joint 6th International IEEE Northeast Workshop on*, pages 49–52. IEEE.
- Uijlings, J. R., Van De Sande, K. E., Gevers, T., and Smeulders, A. W. (2013). Selective search for object recognition. *International journal of computer vision*, 104(2):154–171.
- Usami, H., Hanai, Y., Iwahori, Y., and Kasugai, K. (2016). 3d shape recovery of polyp using two light sources endoscope. In *Computer and Information Science (ICIS), 2016 IEEE/ACIS 15th International Conference on*, pages 1–6. IEEE.
- Winawer, S. J., Fletcher, R. H., Miller, L., Godlee, F., Stolar, M., Mulrow, C., Woolf, S., Glick, S., Ganiats, T., Bond, J., et al. (1997). Colorectal cancer screening: clinical guidelines and rationale. *Gastroenterology*, 112(2):594–642.
- Wu, C., Narasimhan, S. G., and Jaramaz, B. (2010). A multi-image shape-from-shading framework for near-lighting perspective endoscopes. *International Journal of Computer Vision*, 86(2-3):211–228.
- Yang, Q., Tang, J., and Ahuja, N. (2015). Efficient and robust specular highlight removal. *IEEE transactions on pattern analysis and machine intelligence*, 37(6):1304–1311.
- Yang, Q., Wang, S., and Ahuja, N. (2010). Real-time specular highlight removal using bilateral filtering. In *European conference on computer vision*, pages 87–100. Springer.
- Zhang, Z. (2000). A flexible new technique for camera calibration. *IEEE Transactions on pattern analysis and machine intelligence*, 22(11):1330–1334.